Integration of Real-Time Monitoring and Data Analytics to Mitigate Sand Screenouts During Fracturing Operations

Lei Hou[1]*, Derek Elsworth[2], Peibin Gong[3], Xiaobing Bian[4], and Lei Zhang[5]*

[1]China-UK Low Carbon College, Shanghai Jiao Tong University
[2]Energy and Mineral Engineering & Geosciences, EMS Energy Institute and G3 Center, Pennsylvania State University
[3]Drilling Technology Research Institute of SINOPEC, Shengli Oilfield Service Corporation
[4]SINOPEC Research Institute of Petroleum Engineering
[5]School of Petroleum Engineering, China University of Petroleum (East China)

Summary

Sand screenout, the most frequent incident during hydraulic fracturing, is one of the major threats to operational safety and efficiency. Screenout occurs when advancing hydraulic fractures are blocked by injected proppant-slurry, stall, and develop fluid overpressure. Because massive wells are still being hydraulically fractured every year, operational safety has become a critical and urgent issue that has always been overshadowed by the whether-or-not controversy. However, the suddenness and unheralded surprise of screenout make it extremely difficult to predict and handle. Previous efforts attempt to predict screenout as discrete events by interpreting injection pressure directly. We propose and then demonstrate a self-updating (via data and experience augmentation) and customizable (numerical models and algorithms) data-driven strategy of real-time monitoring and management for screenout based on records of shale gas fracturing. Two new indicators—proppant filling index (PFI) and safest fracturing pump rate (SFPR)—are improved and then integrated into the strategy. The PFI reveals the mismatch between injected proppant and hydraulic fractures and provides a continuous time-historical risk assessment of screenout. A pretrained ensemble learning model is applied to process the geological and hydraulic measurements in real time for the PFI evolution curve during fracturing operations. Integrated with the SFPR, a stepwise pump rate regulation strategy is deployed successfully to mitigate sand screenout for field applications. Four field trials are elaborated, which are representative cases exhibiting the data-driven approach to monitor and manage sand screenout during hydraulic fracturing.

Introduction

Hydraulically fractured horizontal wells have accounted for most of all new wells since late 2014 in the United States and for 83% of the total linear footage drilled as of 2016 [about 670,000 wells according to the U.S. Energy Information Administration (2018). During the fracturing operation, sand screenout is one of the most frequent major incidents jeopardizing safe hydraulic fracturing. This is especially the case for unconventional reservoirs using low-viscosity fracturing fluid (e.g., slickwater) (Aud et al. 1994; Barree and Conway 2001; Nolte and Smith 1981). Sand screenout is usually caused by the proppant settling, piling up, and then blocking flow in artificial fractures and thereby stalling the propagating hydraulic fracture tip (Dontsov 2022; Wang and Sharma 2023). The consequent injections of fluids and proppant, therefore, build pressure sharply and threaten the safety around the wellhead. An emergency pump shutdown is usually performed to relieve the wellhead pressure. Meanwhile, the injected proppant may settle down and bury the wellbore, which often requires a suspension of fracturing operations, opening the well for flowback and flushing to clean the wellbore, and then rebuilding the pump rate for the following operation (pumping the perforating gun for the following stages). Therefore, dealing with sand screenout is both a time- and economically consuming process. Forewarning and then mitigating such events is a logical pathway to simultaneously improve both the safety and economic outcomes of fracking.

The direct monitoring and detection of sand screenout events thousands of meters underground are neither mature nor currently economical (Yew and Weng 2014). The provision of expensive microseismic monitoring has not proved successful, as clear signals are difficult to detect and robust diagnostics are even more difficult to define (Li et al. 2019; Warpinski et al. 2012). Advanced fracture-diagnostic techniques (radioactive tracers combined with nuclear logging and fiber-optic sensing, among others) improve the monitoring of fluid/proppant transport through perforation clusters, but it is still challenging to detect the real-time proppant behavior in fractures deep into reservoirs (Shoaibi et al. 2023; Tang et al. 2017; Wu et al. 2021). Screenouts are typically defined as discrete events by manually inspecting the fracturing pressures (Geary et al. 1993; Massaras and Massaras 2012) or by using machine learning algorithms (Ben et al. 2020; Hu et al. 2020; Sun et al. 2020; Yu et al. 2020). One major limitation is that discrete predictions give little lead time to the sudden onset of screenout, thus leaving limited time for the operator to perform remedial measures, even with 100% correct outcomes. The other is the error and bias in the direct interpretation of the fracturing pressure, due to its sensitivity to variations in frictional resistance to flow, proppant settling, and fracture propagation (Daneshy 2007; Nolte 1991; Roussel et al. 2012). Moreover, real-time screenout management is another key issue that is rarely reported because reducing or staunching the pump rate is the sole mitigative action (to a rapid or near-instantaneous jump in fracturing pressure). This action completely depends on the experience of the operator in knowing how quickly or by how much the pump rate should be regulated. Completely stopping flow or applying an inappropriately low pump rate will aggravate screenout by promoting proppant settling and dune creation in the fracture and will also intensify water hammer effects and their damage

*Corresponding author; email: leihou.upc@gmail.com; zhlei@upc.edu.cn

Original SPE manuscript received for review 28 August 2023. Revised manuscript received for review 12 March 2024. Paper (SPE 219747) peer approved 18 March 2024.
Supplementary materials are available in support of this paper and have been published online under Supplementary Data at https://doi.org/10.2118/219747-PA. SPE is not responsible for the content or functionality of supplementary materials supplied by the authors.

to well integrity, exacerbating the problem at restart (Harris and Pippin 2000; Willingham et al. 1993). Therefore, a robust method to define and regulate, in real time, the emergency pump rate is urgently needed.

We propose a new data-driven strategy for the real-time monitoring and management of sand screenout. This method improves and then integrates two key indices that are used for post-fracturing analyses in our previous studies—the PFI (Hou et al. 2023) and the SFPR (Hou et al. 2022a): (i) The PFI (defined as the volume proportion of proppant-filled fractures to the total volume of proppant-accessible fractures) estimates the mismatch between proppant injection and underground fracture propagation in real time. This more accurately reflects the true mechanism of screenout compared with the previous interpretation of surface-measured fluid pressure. A time-continuous PFI curve is produced by a pretrained ensemble learning workflow updated by real-time records. This presents the time histories of the fracturing process compared with previous predictions of discrete events, thus allowing for early warning and then preventative measures. (ii) The SFPR is generated by mining the data from prior screenout cases based on a deep learning workflow combined with sensitivity analyses of the U-shaped correlation between pump rate and screenout probability. This suggests the regulation rate and range required of the pumping to prevent or mitigate screenout. The new strategy can self-update by continuously collecting new cases and data from field applications.

The numerical models and algorithms are the two core techniques of the new strategy, which are customizable and may be improved by fundamental research. In our field trials, the new strategy successfully prevented three screenout events. The high efficiency and broad applicability of this new data-driven method provide an urgently needed technique to monitor and manage sand screenout during hydraulic fracturing.

Methodology

Integrated Strategy and Its Application. A new data-driven strategy and its application for the real-time monitoring and management of sand screenout are proposed as shown in **Fig. 1,** which integrates the PFI and SFPR, data collection, numerical models, and machine learning workflows. Details of hypotheses and definitions of PFI and SFPR are explained in **Fig. 2** and the Supplementary Material. The upper orange-line workflow uses the data from screenout and near-screenout fracturing wells to train an ensemble learning algorithm. This algorithm is pretrained by historical records (Supplementary Material, Tables S-1 and S-2) and then predicts the PFI monitoring curve for the real-time fracturing operation by manually feeding in the real-time measurements. The lower blue-line workflow analyses data from screenout cases and generates a pump rate management strategy (SFPR) for real-time regulation when encountering the screenout to prevent or mitigate the operational risks. The SFPR is fitted based on the U-shaped correlation between pump rate and the screenout probability that was revealed by our previous work (Hou et al. 2022a), as marked in the gray ellipse in **Fig. 2**. In this study, new data and new parameters are introduced. Therefore, the input features are first optimized to verify the U-shaped correlation and then fit the SFPR based on newly collected data, as illustrated in Supplementary Material, Tables S-3 and S-4 and Figs. S-1 through S-4.

This study adopts the definitions but improves the usage of the key indices. For PFI, a new numerical model (considering evolutions of the proppant ridge, Eq. S-5, Supplementary Material) is applied to extract the input feature and then improve the algorithm training. This model upgrade is also an example of the customizable characteristic of the new strategy, as shown in **Fig. 2**. Moreover, the ensemble learning model **(Fig. 2)** for PFI is applied for processing field records and updating the PFI curve in real time, compared with the one-time prediction for post-fracturing analyses in the previous study (Hou et al. 2023). The successful field trials in this study demonstrate and expand the capability of the PFI curve for real-time monitoring, which provides time-sequential histories of underground conditions compared with previous discrete sudden events, thus allowing for early warning and then preventative measures. For SFPR, more elaborate sensitivity analyses are performed in this study. The moderating effects of pore pressure, stage length, fluid viscosity, proppant size, well/vertical depths, and proppant concentration (Supplementary Material) are presented, compared with the previous brief analysis mainly focusing on horizontal stress (Hou et al. 2022a). These in-depth analyses direct the pump rate management for real-time regulation

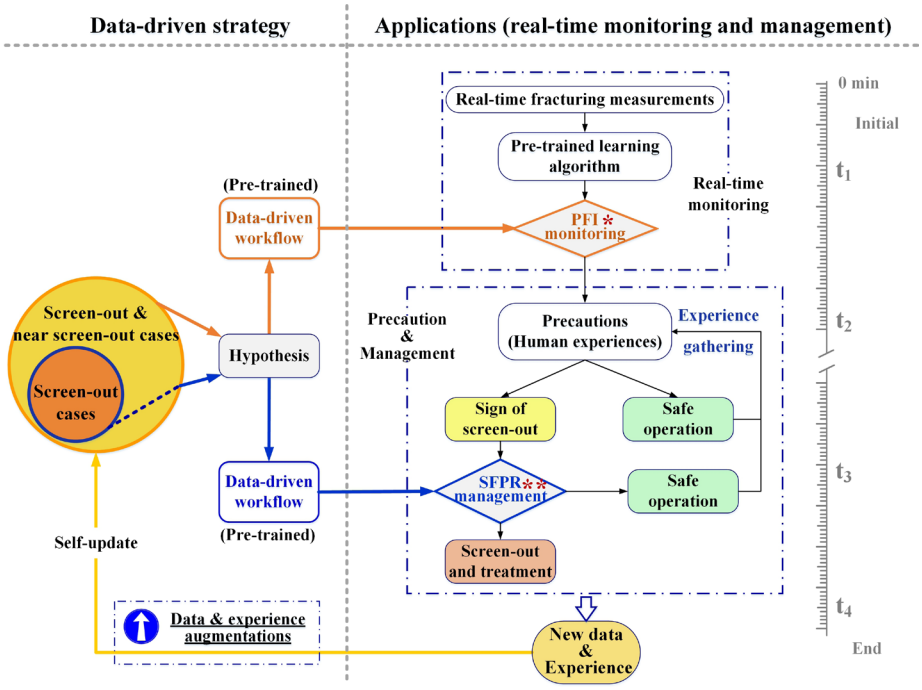

Fig. 1—Structure of the data-driven strategy and its application. The *PFI monitoring and **SFPR management are the pivotal techniques to prevent and mitigate sand screenout in real time.

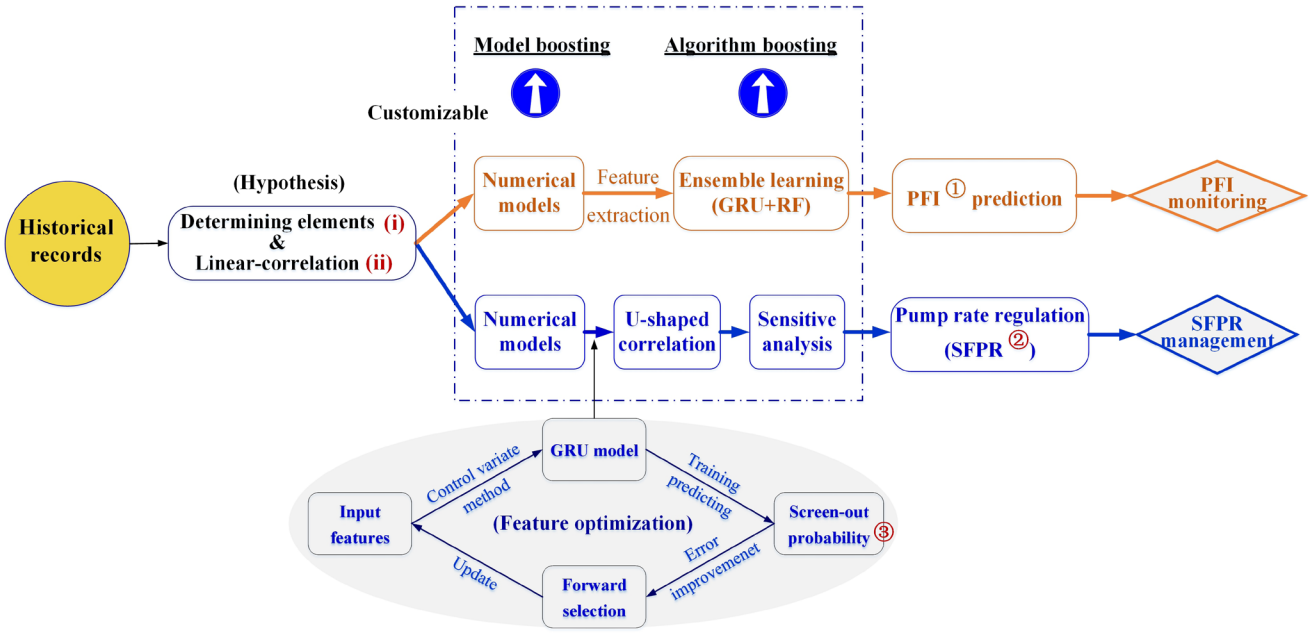

Fig. 2—Pretrained data-driven workflows. New parameters (PFI, SFPR, and screenout probability) are defined based on the (i) determining elements hypothesis and the (ii) linear-correlation hypothesis.

in field pilots, as illustrated in the "Field Trials" section. More importantly, the pump rate adjustments reveal the interconnection between pump rate and real-time PFI evolution, which further generates the new stepwise regulation strategy. Above all, the integration of PFI and SFPR and their successful applications in field trials is one of the major contributions of this study.

Numerical Model and Feature Extraction. Feature extraction by numerical models is the core technique for data augmentation during the preprocessing to improve the performance of trained algorithms (as summarized in the Supplementary Material). The analytical models are optimized to manually calculate features in real time based on the fracturing measurements (per second). The extracted features are summarized in **Table 1**, involving V_s/V_f (the volume ratio of injected sand and fluid), H_1 (the height of the slurry flowing layer in fractures), η (the fluid efficiency in fractures), DPP [the downhole pressure after hole perforation (fracture inlets)], and $\Delta P/\Delta V_f$ (the wellhead pressure change in a unit volume of injected fluid). We considered the generation of a proppant ridge when injecting pure fluid during the estimation of H_1 (Eq. S-5, Supplementary Material) (Hou et al. 2022b), which improves the input features for PFI prediction compared with the previous model (Hou et al. 2023). The fluid efficiency (η) is estimated (for the ongoing fracturing operation) using the fracture closure time of the neighboring wells, as explained in the Supplementary Material (Eq. S-9). In the case study, the hydraulic measurements (pump rate, wellhead pressure, fluid viscosity, proppant diameter, and concentration) are collected and preprocessed (for V_s/V_f, H_1, and η) in the field after every two or three stages of proppant injection (depending on the stage length that allows enough time for data processing). These measurements and extracted features are then applied in the ensemble learning workflow for the real-time PFI curve.

	Inputs for PFI	Inputs for Screenout Probability
Original Features	Extracted Features	Extracted Features
Well depth; vertical depth; minimum horizontal stress; pore pressure; stage number; stage length pump rate; wellhead pressure fluid viscosity; proppant diameter and concentration	V_s/V_f H_1 η	DPP V_s/V_f $\Delta P/\Delta V_f$

Notes: V_s/V_f = volume ratio of injected sand and fluid; H_1 = height of the slurry flowing layer in fractures; η = fluid efficiency in fractures; DPP downhole pressure after hole perforation; $\Delta P/\Delta V_f$ = wellhead pressure change in a unit volume of injected fluid.

Table 1—Summary of inputs for predicting PFI and screenout probability.

Data and Algorithm. The field measurements of shale gas fracturing wells are collected from the southeast region of the Sichuan Basin, China, representing data from 29 fracturing stages (more than 286,000 groups of fracturing records in seconds) from 18 wells. Ten of the collected stages (from nine wells) encountered screenout (the fracturing operation is suspended to release pressure), and the rest are near-screenout cases (the condition of encountering rapid pressure rise, mandating pump rate reduction, but succeeding in subsequent operations). The data set includes geological and hydraulic parameters (the "Original Features," as summarized in **Table 1**) based on previous studies on proppant transport in subsurface fractures (Hou et al. 2022a, 2022b).

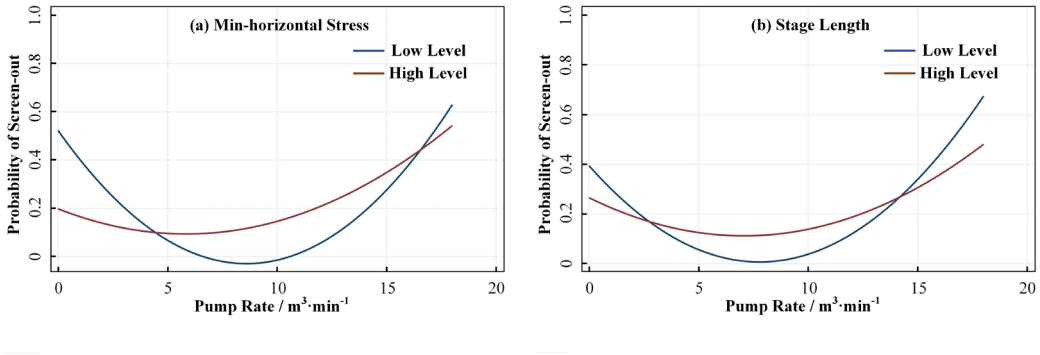

Fig. 3—Moderating effects of parameters on the U-shaped correlation between pump rate and screenout probability. The U-shaped curves are plotted under low (mean – 1 standard deviation) and high (mean + 1 standard deviation) levels of (a) minimum horizontal stress and (b) stage length.

Two gate recurrent unit (GRU) models with three layers (including the output layer) are built for predicting both screenout probability and PFI, using the "ReLu" as the activation function in each layer and based on previous experience (Hou et al. 2022a, 2022b). The Adam routine is selected as the optimizer to compile the model, where a callback function is applied to return and automatically update the learning rate (Kingma and Ba 2014; Zeiler 2012). The regularization is performed to avoid overfitting by setting a dropout (of 0.2) behind the first and hidden layers. All the original field measurements are used as the inputs for model tuning. The hyperparameters, including the number of neural nodes in each layer, the batch size, and epochs, are optimized by the Grid search and walk-forward validation (Bergstra and Bengio 2012; Hu et al. 1999). The Grid search expects the input in two dimensions. Therefore, we add an extra layer before the input layer to temporarily reshape the matrix into three dimensions in the GRU model. The walk-forward validation preserves temporal components inherent in the time-series problem (Stein 2002), which is suitable for evaluating our model. The process of algorithm tuning is presented in the Supplementary Material (Tables S-1 and S-2). The GRU model for predicting screenout probability is tuned with screenout cases only, while the model for predicting PFI is tuned with the entire data set. A random forest regression algorithm with 50 estimators is also built to improve the predictions. The GRU and random forest algorithms are ensembled using a simple average strategy—averaging the predictions of these two algorithms as eventual outcomes.

Results and Discussion

Sensitivity Analyses for SFPR. Sensitivity analyses are performed to define the moderating effects of the optimized parameters (including the well and vertical depth, stage length, pore pressure, minimum horizontal stress, fluid viscosity, and proppant concentration and diameter) on the U-shaped correlation and to characterize the evolution of the SFPR under various conditions (**Figs. 3 and 4,** and Figs. S-1–S-4, Supplementary Material). The representative results (minimum horizontal stress, stage length, fluid viscosity, and proppant diameter) are shown in **Figs. 3 and 4**. The SFPR migrates rightward under low-stress conditions (mean – 1 standard deviation) and moves leftward under high-stress conditions (mean + 1 standard deviation). The variation of the SFPR falls in the range between 5 m^3/min and 10 m^3/min (31.45 bbl/min and 62.90 bbl/min) in **Fig. 3a**. Similar rules are observed in the moderating effects of well and vertical depth and pore pressure (Supplementary Material, Figs. S-2 and S-3). In **Fig. 3b**, a shorter stage length results in a lower probability of screenout in the commonly applied range of pump rate between 3 m^3/min and 15 m^3/min (18.87 bbl/min and 94.35 bbl/min), which may benefit from constraining fluid distributions through smaller perforation holes and thus boosting the development of fractures in reservoirs. This correlation, however, reverses (longer stage length results in a lower probability) when the pump rate exceeds 15 m^3/min (94.35 bbl/min), which may benefit from the provision of more perforation holes (through the casing) that may lessen the pressure buildup under the high-pump-rate condition.

A different method is deployed to analyze the moderating effect of fluid viscosity, proppant concentration, and diameter, due to the discrete nature of these data. We test the U-shaped correlation under different fluid and proppant conditions that represent typical values

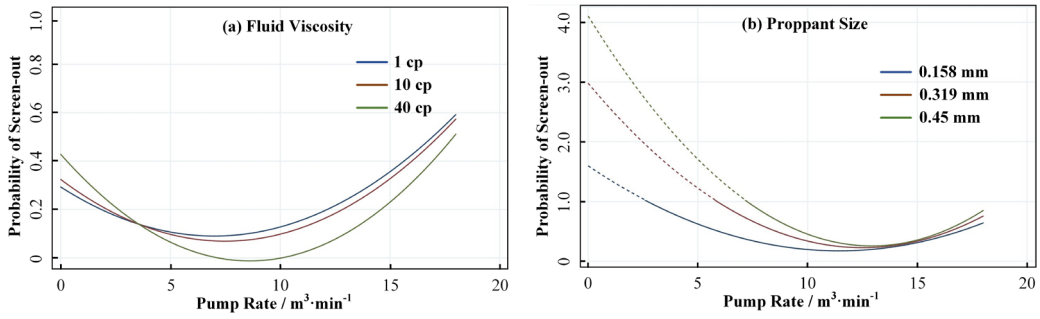

Fig. 4—Moderating effects of parameters on the U-shaped correlation between pump rate and screenout probability. The U-shaped curves are plotted under representative values of (a) fluid viscosity and (b) proppant size due to their discrete data characteristics.

of these parameters based on the collected field data. Increasing fluid viscosity reduces settling rates of the proppant and improves proppant transport along the fracture, thus diminishing the screenout probability **(Fig. 4a)**. The increasing proppant size and concentration move the SFPR rightward, approaching 15 m^3/min (94.35 bbl/min) and also increasing the probability and the slope (**Fig. 4b** and Fig. S-4, Supplementary Material). The proppant parameters reflect the stage in the fracturing procedure because large-diameter proppants and high concentrations are used near the end of the fracturing operation. A higher pump rate is essential to maintain the slurry flow in the created fracture and continue the fracturing operation.

To summarize, the suggested SFPR range for the targeted region falls between 5 m^3/min and 10 m^3/min (31.45 bbl/min and 62.90 bbl/min). Pump rate regulation (both increasing and decreasing) should be moderated according to the variation in the slope of the probability curve. However, the fracturing pressure may still jump dramatically when encountering screenout, leaving limited time to quantify the necessary reduction in pump rate. We, therefore, integrate the PFI real-time monitoring with SFPR for field application.

Field Trials. The new strategy, integrating PFI and SFPR, is prepared for field trails in the same region as the sourced data. Four representative field applications are summarized in **Figs. 5 through 8.** The injection parameters and wellhead pressure are fed into the pretrained ensemble learning workflow in real time for the prediction of PFI **(Fig. 1)**. This predictive algorithm was applied manually using real-time rig data to provide a real-time PFI curve (combined with hydraulic measurements, as listed in **Table 1**) to allow the field engineers to monitor the fracturing operation. The PFI curve keeps growing along with the time when the real-time data accumulates and is applied continuously in the ensemble learning workflow, as presented in **Figs. 5 through 8**. We indexed the imminent risk of sand screenout to when the PFI curve grew rapidly or remained high (>80). The field engineers decided whether to take preventive action or not based on our suggestion and their experience. Similarly, we suggested the SFPR emergency strategy (gradually reducing the pump rate down to 5–10 m^3/min according to the sensitivity analyses) with the field operators improvising based on our preplan and their observational judgment when encountering the signs of screenout (a sharp increase of wellhead pressure). We present the PFI evolution curve at the beginning (t_1), in the middle (t_2, t_3), and at the end (t_4) of the fracturing process. The regulation applied to the pump rate, trying to manage the screenout, is magnified on the right side of **Figs. 5 through 8** to illustrate the regulation strategy.

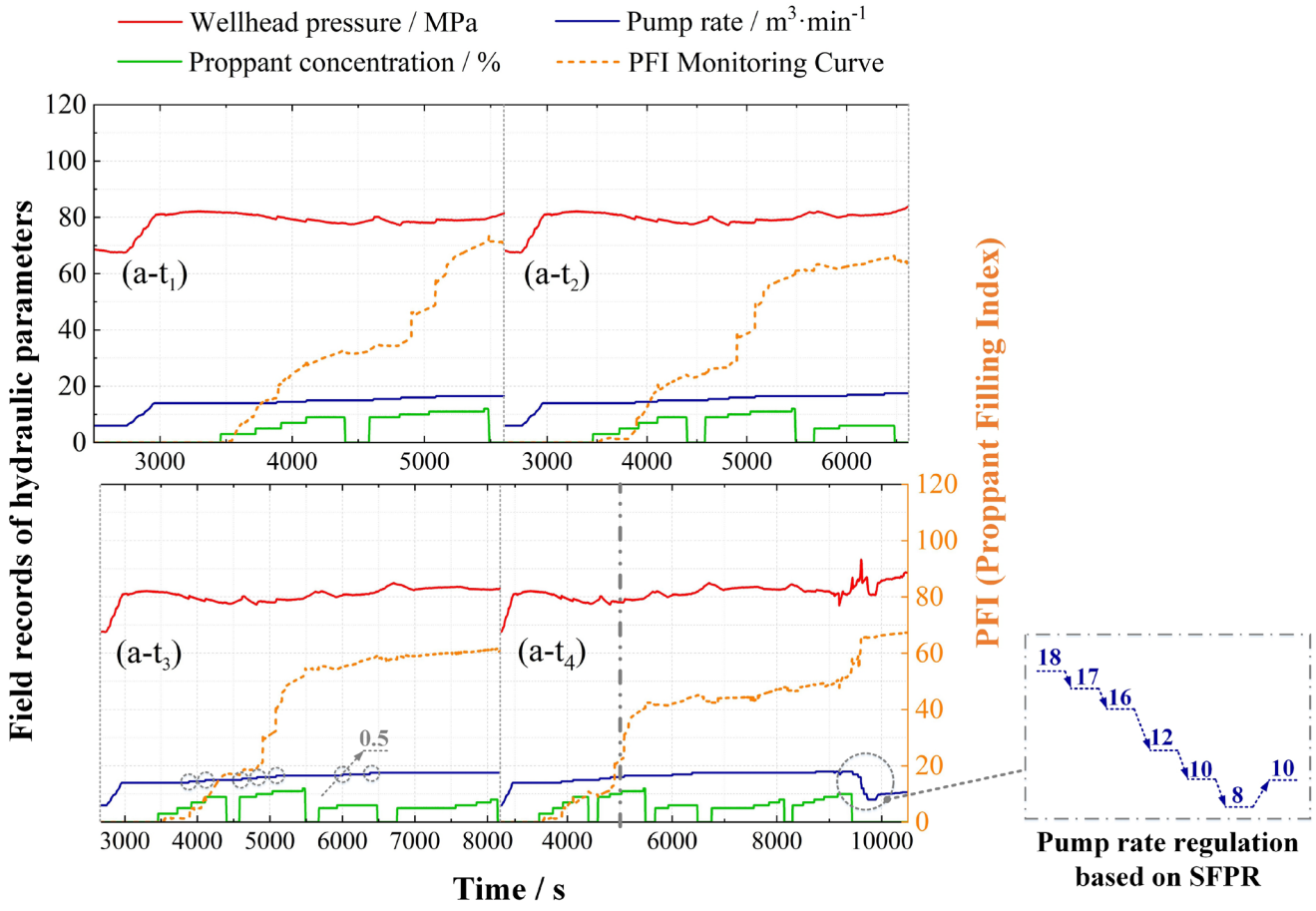

Fig. 5—PFI monitoring and SFPR management for Case 1 (Well A). The vertical dashed-dotted lines mark the PFI jumps due to the proppant injection. The dashed circles (t_4) and connected dashed-dotted rectangles represent the pump rate regulation, referring to SFPR.

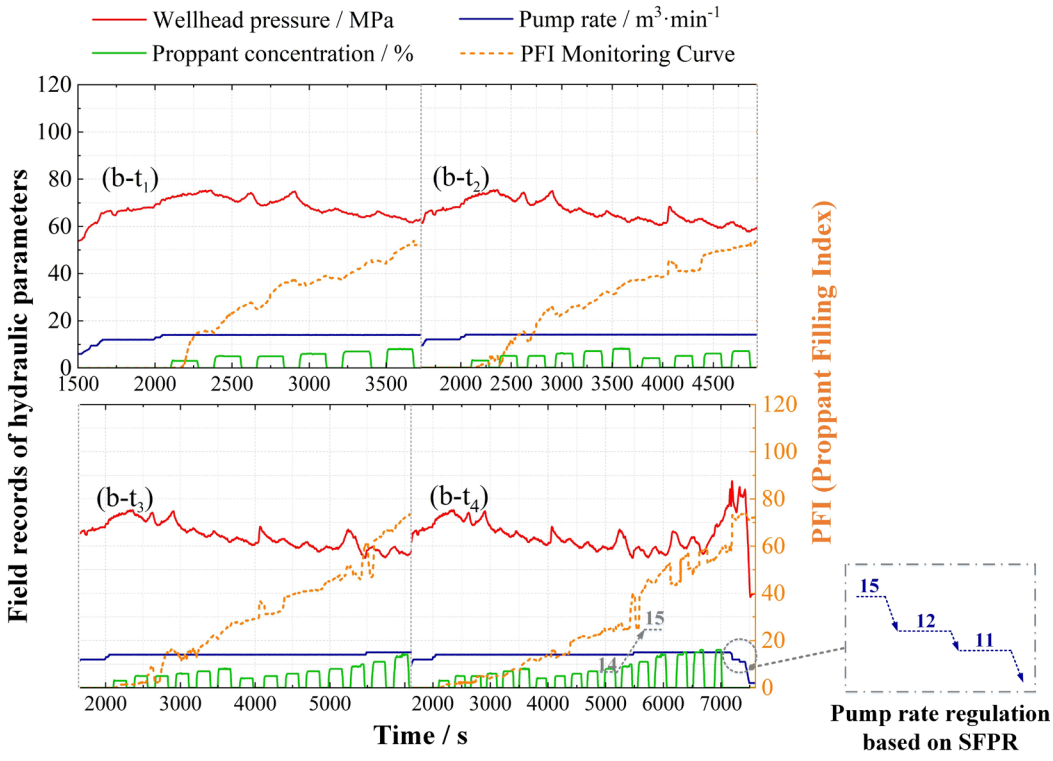

Fig. 6—PFI monitoring and SFPR management for Case 2 (Well B). The dashed polylines and numbers at time t_4 mark the increases in pump rate that induce fluctuations in PFI. The dashed circles and connected dashed-dotted rectangles represent the pump rate regulation, referring to SFPR.

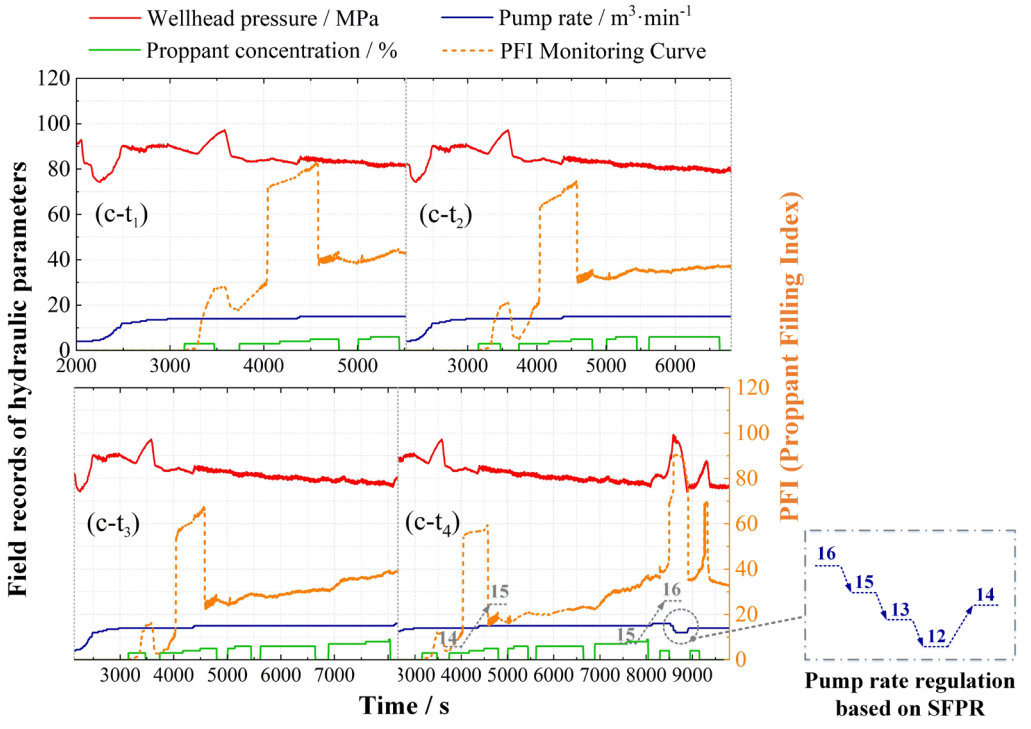

Fig. 7—PFI monitoring and SFPR management for Case 3 (Well C). The dashed polylines and numbers at time t_4 mark the increases in pump rate that induce fluctuations in PFI. The dashed circles and connected dashed-dotted rectangles represent the pump rate regulation, referring to SFPR.

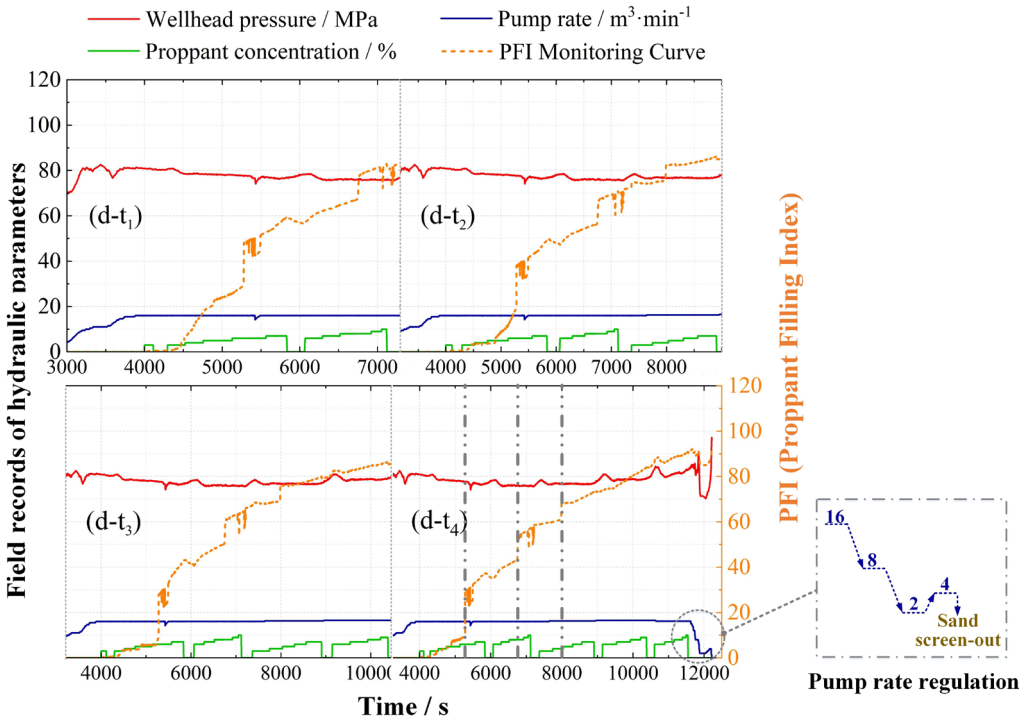

Fig. 8—Sand screenout case (Case 4, Well D) failed to follow the instructions of PFI monitoring. The vertical dashed-dotted lines mark the PFI jumps due to the proppant injection. The dashed circles (t_4) and connected dashed-dotted rectangles represent the emergency pump rate regulations.

Case 1 (Well A) is a successful application of our new strategy, as shown in **Fig. 5**. The proppant was injected near continuously (discrete green curves at the bottom), indicating a low operating difficulty for a shale gas well. However, the PFI reported a sharp increase during the second proppant injection slug, at ~5,000 seconds (labeled by the vertical dashed-dotted line in **Fig. 5**, a-t_4). We, therefore, reduced the proppant concentration and volume in the following slug of proppant injection, referring to the high sensitivity of screenout probability to the proppant parameters **(Fig. 4b)**. The proppant concentration afterward was also reduced, as represented by the flat trend of the PFI curve thereafter. The signs of screenout appeared after the proppant injection. We stepwise reduced the pump rate from 18 m^3/min (113.22 bbl/min) down to 8 m^3/min (50.32 bbl/min), falling in the recommended range of SFPR (5~10 m^3/min). Finally, a pump rate of 10 m^3/min (62.90 bbl/min) was reestablished to finish this fracturing operation.

Case 2 (Well B) is a fracturing operation in a shallower subdivided formation, thus requiring lower wellhead pressure **(Fig. 6)**. The PFI grew smoothly before ~5,500 seconds in this case and then rose sharply after a pump rate increase [from 14 m^3/min to 15 m^3/min (88.06 bbl/min to 94.35 bbl/min)] as labeled in **Fig. 6** (b-t_4). A sharp jump in vertical pressure (a sign of screenout) emerged at the end of the fracturing operation. We gradually decreased the pump rate and maintained it at ~11 m^3/min (69.19 bbl/min) because of the high proppant concentration (15~16% in the end) requiring a relatively high pump rate as suggested by Fig. S-4, Supplementary Material. The pressure became controllable at ~11 m^3/min until the end of operations when sufficient pure fluid had been injected to clean up the wellbore.

Case 3 (Well C) further exhibited the effect of increasing pump rate on the evolution of PFI, as shown in **Fig. 7**. The pump rate was maintained at 14 m^3/min (88.06 bbl/min) initially and then was boosted to 15 m^3/min (94.35 bbl/min) and then 16 m^3/min (100.64 bbl/min) at 4,500 seconds and 8,000 seconds, respectively **(Fig. 7**, c-t_4). Dramatic fluctuations in PFI were observed after applying these pump rate increases, as well as a reversal in the trend of pressure change from decreasing to increasing at ~8,000 seconds. This feature is indicative of proppant settling within the fracture and depositing a "dune" falling from the injection point (Hou et al. 2022b) and due to density differences within the fracturing fluid. The flowing channel above the dune then controls the frictional resistance to flow and the pressure variations. The increased pump rate boots the drag force acting on the surface of the dune, eroding and then depositing a proppant ridge (as presented in **Fig. 8** in the "Discussion" section). The proppant ridge blocked the flowing channel and increased the frictional resistance to flow, thus inducing an increase in pressure after ~8,000 seconds in **Fig. 7**, c-t_4. Notably, the pump rate was increased during, or directly following, the proppant injections in **Fig. 7**, which may promote the generation of such a proppant ridge. The evolution of such ridges is suggested by previous studies combining experiments, deep learning algorithms, and field measurements (Hou et al. 2022b). A similar stepwise relief in pump rate was performed to avoid serious screenout in this case, as shown in **Fig. 7**.

Sand screenout happens in Case 4 (Well D) at the end of the fracturing operation around 12,000 seconds, as shown in **Fig. 8**. During this operation, the field engineering decided to ignore the warning of the PFI curve because of the declining trend of fracturing pressure. The long proppant injection slugs also indicate a well-developed fracture network that may have reduced the risks and difficulties in proppant injection. These superficial phenomena have confused the field operators, causing them to stick to the pumping schedule even though the PFI curve reported three vertical jumps around 5,000 seconds, 7,000 seconds, and 8,000 seconds (as labeled in **Fig. 8**, d-t_4). No prevention measures were performed when the PFI exceeded 80 around 10,000 seconds **(Fig. 8**, d-t_4). Therefore, a festinate pump rate cutdown was carried out but failed to reestablish the pump rate due to the vertical increase of wellhead pressure—a typical case of sand screenout.

Recommendations to Field Applications. Rapid increases in the PFI prewarn of an impending screenout, even under deceptive conditions when the wellhead pressure is constant **(Fig. 5)** or declining **(Figs. 6 and 8)**. The initial prediction of PFI (at t_1 in **Figs. 5 through 8**) steps down, by feeding in subsequent new data, with time from t_1 to t_4, which reflects characteristics in the development of the

evolving subsurface fracture network. Several effective measures are summarized as mitigative actions derived from human experience, based on **Figs. 5 through 8**.

Reducing the concentration and volume of proppant in a single slug and increasing the pump rate can be useful to rebalance the proppant injection and fracture propagation **(Fig. 5)**. The monitoring of the PFI curve supports first-time adjustments to the pump schedule slug by slug, which is ground-breaking compared with traditional adjustment stage by-stage.

A stepwise pump rate regulation is generated based on the successful prevention of serious screenout in three cases and the sensitivity of PFI by pump rate variations (**Figs. 5 through 7**). Advance warning from the PFI must be sufficient to allow the reaction to reduce pump rate and therefore manage against screenout

The pump rate should be increased only slowly to avoid screenout due to the potential for deformation of the proppant dune within the fracture, as illustrated in **Fig. 9.** When the pump rate is increased, the increased frictional drag may re-entrain the settled proppant to form a proppant ridge **(Fig. 9b)**. An obstructed flowing channel (from H_1 to H_1' in **Fig. 9**) increases the frictional flow resistance to subsequent injections, thereby changing wellhead pressure and inducing sand screenout (Hou et al. 2022b). **Figs. 6 and 7** suggest that an increase in the pump rate of 1 m^3/min (6.29 bbl/min) may induce significant variation in PFI, which agrees with the higher sensitivity of screenout probability under high-pump-rate conditions **(Fig. 3)**. Regulation using only half of this increment [0.5 m^3/min (3.15 bbl/min)] is recommended, referring to **Fig. 5**, in which frequent but only small adjustments (between 3,500 seconds and 6,500 seconds) are reflected in only slight variations in the PFI curve.

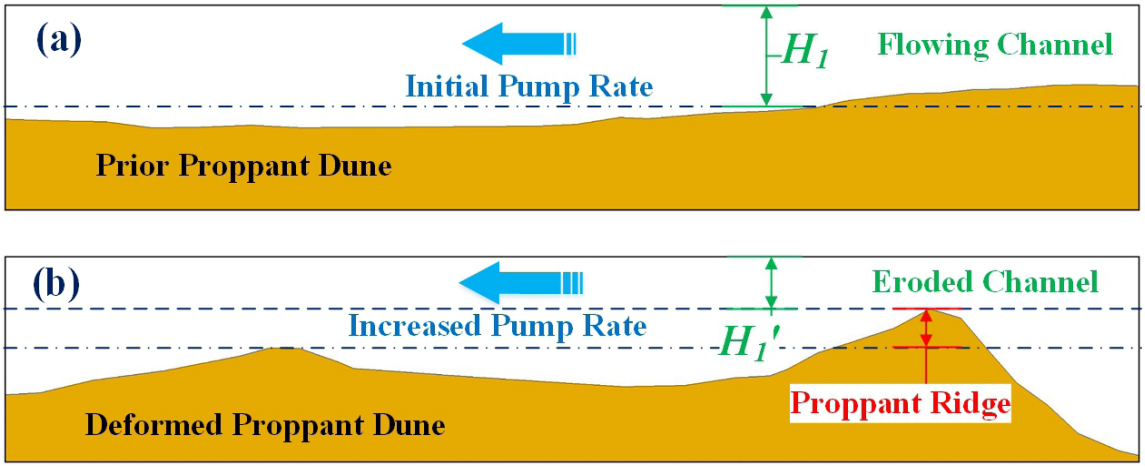

Fig. 9—Schematic of proppant dune evolution by the pump rate increase. (a) H_1 represents the height of the flowing channel in fractures. (b) This height is eroded (H_i') by the increased pump rate that deforms the proppant dune and generates a ridge. Reproduced with permission from Hou et al. (2022b).

Notably, the safety window between fracturing pressure and wellhead capacity should be the most important basis for a decision. An emergency shutdown may be mandatory if the safety window is too narrow in order to ensure the safety of both health and the environment.

Applicability of the New Strategy. We use machine learning algorithms to extract experiences from previous cases to evaluate and manage the risk of ongoing cases—this is the structure and logic of our new strategy. Data labeling (for dependent variables during the algorithm training) is the main challenge of this new method because the direct underground detection of proppant injection is currently unavailable. The PFI defines the threshold between screenout cases and regular cases, which is the basis for the risk assessment. We specifically design the structure of this new method to maximize its applicability.

In particular, the new method requires a relatively small-scale data set to produce satisfactory outcomes (**Figs. 5 through 8**). Only 18 wells are involved in the training before application in our field trials. This is an easy data threshold to meet because a regular field usually includes thousands of wells. Even in the early stages of development, the available data may be used and augmented as experience builds. The method will self-update with the augmented data, even if a successful mitigation strategy has not become apparent—a natural benefit of machine learning algorithms (Goodfellow et al. 2016).

The input features and algorithm of the data-driven workflow are customizable according to the experiences of a targeted field and may be improved with developments in fundamental research. Additional index parameters (e.g., the elasticity of fracturing fluids) may be recorded, as available, and incorporated into the algorithm. The development of more advanced numerical models (e.g., the new Eq. S-5 for H_1 in the Supplementary Material) and more perceptive machine learning algorithms will boost the fidelity of the workflows. Moreover, the application of this strategy is only recommended in the same region as the sourced data for algorithm training to mitigate the uncertainties in engineering and geological conditions and operators.

We balance the human-machine interaction in this strategy for human intervention because the management of screenout is also highly dependent on the judgment and speed of reaction of operators. The sand screenout case (Case 4 in **Fig. 8**) presents a negative example to show the role of the human element. The PFI and SFPR indices are designed as references to aid (rather than replace) humans in making decisions and gaining experience **(Fig. 1)**, which is another form of the self-updating characteristics of this method by integrating human intelligence and learning.

Limitations and Implications

Certain simplifications (of fracture complexity and ignoring the fracture propagation during proppant injection) are applied only for manually calculating the PFI (by Eq. S-1, Supplementary Material) for the screenout and near-screenout cases. For all other regular cases, the PFI is predicted by the ensemble-learning algorithm that is free from any dependence on these simplifications or assumptions. Notably,

we integrated numerical models into the machine-learning workflow to extract more features (fluid efficiency, proppant settling, etc.) than the manual calculation for training the algorithm, which improves the accuracy of the predicted PFI. Other simplifications include the constant physical properties of fracturing fluids represented by the viscosity. We ignore the influence of formation temperature, high-speed injection, and formation water salinity on the fluid properties. Further studies may investigate the real fluid properties under formation conditions, as well as the varying fluid performances in leakoff and proppant transport.

The factors influencing sand screenout are complex. Previous work on conventional reservoirs suggests that the near-wellbore tortuosity of fractures may also play an important role in causing screenout, in addition to fluid leakoff, reactivation of natural fractures or faults in shear, issues of fluid quality or surface equipment, and other factors (Aud et al. 1994; Barree and Conway 2001; Daneshy 2007). However, for the fracturing of unconventional reservoirs, the acid spearhead and fine (100-mesh) proppant are usually injected to erode, straighten, and thereby reduce (improve) the near-wellbore tortuosity. The ultralow permeability of unconventional reservoirs also reduces the fluid leakoff. Thus, we posit that the mismatch between proppant injection and fracture propagation (evaluated by the PFI) becomes the major mechanism contributing to sand screenout in unconventional reservoirs.

Moreover, the PFI monitoring strategy is designed to aid (rather than replace) humans in managing the screenout. Human intelligence is essential during the application of this strategy (as shown in **Fig. 1**) to synthetically judge the factors promoting a sand screenout event. For instance, the pump rate increase during proppant injection induces significant fluctuations in FPI curves, as observed in Cases 2 and 3 (with an amplitude of 1 m^3/min). However, increasing the pump rate slowly with an amplitude of 0.5 m^3/min reports minor influences on the PFI curve in Case 1, which was summarized as an important human experience for elaborate regulations of pump rate. This is a representative example of combining human and artificial intelligence to secure fracturing operations. Other field practices preventing sand screenout include the applications of lightweight proppant or higher-viscosity fluids, and injecting a longer pure-fluid pad between proppant pads, among others (Biheri and Imqam 2023; Siddhamshetty et al. 2018; Wood et al. 2003).

Conclusions

Sand screenout is a frequent but highly underrated issue for both operational safety and economic loss during hydraulic fracturing for shale oil/gas. We propose a self-updating and customizable data-driven strategy to produce a real-time risk assessment (PFI curves) and inform the management (SFPR pump rate regulation) of screenout. This compares with previous efforts that predict screenout as discrete events a posteriori. Four field applications demonstrate the performance and potential of the new data-driven method for securing hydraulic fracturing operations. This new strategy is designed as a reference to aid (rather than replace) humans in making decisions with the help of machine learning (for PFI) and data mining (for SFPR) techniques. Several effective measures are summarized as mitigative actions against sand screenout based on field trials:

1. Reducing the concentration and volume of proppant in a single slug can be useful when the PFI monitoring curve reports a prewarning (rapid increases) of an impending screenout.
2. A stepwise pump rate regulation is generated, which can mitigate screenout with the help of advance warning from the PFI curve (allowing the reaction to gradually reduce the pump rate).
3. Increasing the pump rate should be performed slowly (an increment of 0.5 m^3/min is recommended based on case studies) to mitigate the deformation of the proppant dune that may obstruct the flow in fractures and cause sand screenout.

Nomenclature

H_1 = height of the slurry flowing layer in fractures
V_s/V_f = volume ratio of injected sand and fluid
$\Delta P/\Delta V_f$ = wellhead pressure change in a unit volume of injected fluid
η = fluid efficiency in fractures

Acknowledgments

This research is funded by the National Natural Science Foundation of China under grant 42377138. DE acknowledges support from the G. Albert Shoemaker endowment.

References

Aud, W. W., Wright, T. B., Cipolla, C. L. et al. 1994. The Effect of Viscosity on Near-Wellbore Tortuosity and Premature Screenouts. Paper presented at the SPE Annual Technical Conference and Exhibition, New Orleans, Louisiana, USA, 25–28 September. https://doi.org/10.2118/28492-MS.

Barree, R. D. and Conway, M. W. 2001. Proppant Holdup, Bridging, and Screenout Behavior in Naturally Fractured Reservoirs. Paper presented at the SPE Production and Operations Symposium, Oklahoma City, Oklahoma, USA, 24–27 March. https://doi.org/10.2118/67298-MS.

Ben, Y., Perrotte, M., Ezzatabadipour, M. et al. 2020. Real-Time Hydraulic Fracturing Pressure Prediction with Machine Learning. Paper presented at the SPE Hydraulic Fracturing Technology Conference and Exhibition, The Woodlands, Texas, USA, 4–6 February. https://doi.org/10.2118/199699-MS.

Bergstra, J. and Bengio, Y. 2012. Random Search for Hyper-Parameter Optimization. *J Mach Learn Res* **13** (2). https://doi.org/https://dl.acm.org/doi/10.5555/2188385.2188395.

Biheri, G. and Imqam, A. 2023. In-Depth Laboratory Proppant Transport Study Using HVFRs for Marcellus High TDS Environments. *SPE J.* **28** (5): 2130–2147. https://doi.org/10.2118/214692-PA.

Daneshy, A. A. 2007. Pressure Variations Inside the Hydraulic Fracture and Their Impact on Fracture Propagation, Conductivity, and Screenout. *SPE Prod & Oper* **22** (1): 107–111. https://doi.org/10.2118/95355-PA.

Dontsov, E. V. 2022. Analysis of a Constant Height Hydraulic Fracture Driven by a Power-Law Fluid. *Rock Mechan Bull* **1** (1): 100003. https://doi.org/10.1016/j.rockmb.2022.100003.

Geary, M. P., Johnson, D. E., Kogsbøll, H.-H. et al. 1993. Field Implementation of Proppant Slugs to Avoid Premature Screen-Out of Hydraulic Fractures with Adequate Proppant Concentration. Paper presented at the Low Permeability Reservoirs Symposium, Denver, Colorado, USA, 26–28 April. https://doi.org/10.2118/25892-MS.

Goodfellow, I., Bengio, Y., Courville, A. et al. 2016. *Deep Learning*. Cambridge, Massachusetts, USA: MIT Press.

Harris, P. C. and Pippin, P. M. 2000. High-Rate Foam Fracturing: Fluid Friction and Perforation Erosion. *SPE Prod & Fac* **15** (1): 27–32. https://doi.org/10.2118/60841-PA.

Hou, L., Cheng, Y., Elsworth, D. et al. 2022a. Prediction of the Continuous Probability of Sand Screenout Based on a Deep Learning Workflow. *SPE J.* **27** (3): 1520–1530. https://doi.org/10.2118/209192-PA.

Hou, L., Cheng, Y., Wang, X. et al. 2022b. Effect of Slickwater-Alternate-Slurry Injection on Proppant Transport at Field Scales: A Hybrid Approach Combining Experiments and Deep Learning. *Energy* **242**. https://doi.org/10.1016/j.energy.2021.122987.

Hou, L., Elsworth, D., Zhang, F. et al. 2023. Evaluation of Proppant Injection Based on a Data-Driven Approach Integrating Numerical and Ensemble Learning Models. *Energy* **264**. https://doi.org/10.1016/j.energy.2022.126122.

Hu, J., Khan, F., Zhang, L. et al. 2020. Data-Driven Early Warning Model for Screenout Scenarios in Shale Gas Fracturing Operation. *Comput Chem Eng* **143**: 107116. https://doi.org/10.1016/j.compchemeng.2020.107116.

Hu, M. Y., Zhang, G. (Peter), Jiang, C. X. et al. 1999. A Cross-Validation Analysis of Neural Network Out-of-Sample Performance in Exchange Rate Forecasting. *Decis Sci* **30** (1): 197–216. https://doi.org/10.1111/j.1540-5915.1999.tb01606.x.

Kingma, D. P. and Ba, J. 2014. Adam: A Method for Stochastic Optimization. arXiv:1412.6980 (preprint; last revised 30 January 2017). https://doi.org/10.48550/arXiv.1412.6980.

Li, L., Tan, J., Wood, D. A. et al. 2019. A Review of the Current Status of Induced Seismicity Monitoring for Hydraulic Fracturing in Unconventional Tight Oil and Gas Reservoirs. *Fuel* **242**: 195–210. https://doi.org/10.1016/j.fuel.2019.01.026.

Massaras, L. V. and Massaras, D. V. 2012. Real-Time Advanced Warning of Screenouts With the Inverse Slope Method. Paper presented at the SPE International Symposium and Exhibition on Formation Damage Control, Lafayette, Louisiana, USA, 15–17 February. https://doi.org/10.2118/150263-MS.

Nolte, K. G. 1991. Fracturing-Pressure Analysis for Nonideal Behavior. *J Pet Technol* **43** (2): 210–218. https://doi.org/10.2118/20704-PA.

Nolte, K. G. and Smith, M. B. 1981. Interpretation of Fracturing Pressures. *J Pet Technol* **33** (9): 1767–1775. https://doi.org/10.2118/8297-PA.

Roussel, N. P., Manchanda, R., and Sharma, M. M. 2012. Implications of Fracturing Pressure Data Recorded during a Horizontal Completion on Stage Spacing Design. Paper presented at the SPE Hydraulic Fracturing Technology Conference, The Woodlands, Texas, USA, 6–8 February. https://doi.org/10.2118/152631-MS.

Shoaibi, S., Farsi, S., Suchta, B. et al. 2023. Fluid and Proppant Distribution and Fracture Geometry Calibration Using Permanent Fiber-Optic Sensing DAS/DTS – Oman Case Study. Paper presented at the SPE/IATMI Asia Pacific Oil & Gas Conference and Exhibition, Jakarta, Indonesia, 10–12 October. https://doi.org/10.2118/215487-MS.

Siddhamshetty, P., Narasingam, A., Liu, S. et al. 2018. Feedback Control of Proppant Bank Heights during Hydraulic Fracturing for Enhanced Productivity in Shale Formations. In *Computer Aided Chemical Engineering*, eds. M. R. Eden, M. G. Ierapetritou, and G. P. Towler, Vol. 44, 703–708. Amsterdam, Netherlands: Elsevier. https://doi.org/10.1016/B978-0-444-64241-7.50112-9.

Stein, R. M. 2002. *Benchmarking Default Prediction Models: Pitfalls and Remedies in Model Validation*. New York, USA: Moody's KMV.

Sun, J. J., Battula, A., Hruby, B. et al. 2020. Application of Both Physics-Based and Data-Driven Techniques for Real-Time Screen-Out Prediction with High Frequency Data. Paper presented at the SPE/AAPG/SEG Unconventional Resources Technology Conference, Virtual, 20–22 July. https://doi.org/10.15530/urtec-2020-3349.

Tang, H., Killough, J. E., Heidari, Z. et al. 2017. A New Technique To Characterize Fracture Density by Use of Neutron Porosity Logs Enhanced by Electrically Transported Contrast Agents. *SPE J.* **22** (4): 1034–1045. https://doi.org/10.2118/181509-PA.

U.S. Energy Information Administration. 2018. Hydraulically Fractured Horizontal Wells Account for Most New Oil and Natural Gas Wells. https://www.eia.gov/todayinenergy/detail.php?id=34732.

Wang, H. and Sharma, M. M. 2023. Uniquely Determine Fracture Dimension and Formation Permeability from Diagnostic Fracture Injection Test. *Rock Mechan Bull* **2** (2): 100040. https://doi.org/10.1016/j.rockmb.2023.100040.

Warpinski, N. R. R., Du, J., and Zimmer, U. 2012. Measurements of Hydraulic-Fracture-Induced Seismicity in Gas Shales. *SPE Prod & Oper* **27** (3): 240–252. https://doi.org/10.2118/151597-PA.

Willingham, J. D., Tan, H. C., and Norman, L. R. 1993. Perforation Friction Pressure of Fracturing Fluid Slurries. Paper presented at the Low Permeability Reservoirs Symposium, Denver, Colorado, USA, 26–28 April. https://doi.org/10.2118/25891-MS.

Wood, W. D., Brannon, H. D., Rickards, A. R. et al. 2003. Ultra-Lightweight Proppant Development Yields Exciting New Opportunities in Hydraulic Fracturing Design. Paper presented at the SPE Annual Technical Conference and Exhibition, Denver, Colorado, USA, 5–8 October. https://doi.org/10.2118/84309-MS.

Wu, K., Liu, Y., Jin, G. et al. 2021. Fracture Hits and Hydraulic-Fracture Geometry Characterization Using Low-Frequency Distributed Acoustic Sensing Strain Data. *J Pet Technol* **73** (7): 39–42. https://doi.org/10.2118/0721-0039-JPT.

Yew, C. H. and Weng, X. 2014. *Mechanics of Hydraulic Fracturing*. Oxford, UK: Gulf Professional Publishing.

Yu, X., Trainor-Guitton, W., and Miskimins, J. 2020. A Data Driven Approach in Screenout Detection for Horizontal Wells. Paper presented at the SPE Hydraulic Fracturing Technology Conference and Exhibition, The Woodlands, Texas, USA, 4–6 February. https://doi.org/10.2118/199707-MS.

Zeiler, M. D. 2012. ADADELTA: An Adaptive Learning Rate Method. arXiv:1212.5701 (preprint; submitted 22 December 2012). https://doi.org/10.48550/arXiv.1212.5701.